International Journal of Engineering and Technology Innovation, vol. 6, no. 4, 2016, pp. 243 - 254

Gear Fault Diagnosis Based on Narrowband Demodulation with Frequency Shift and Spectrum Edit

Yu Guo, Qian-Nan Liu, Xing Wu*, Jing Na

Faculty of Mechanical and Electrical Engineering, Kunming University of Science and Technology, Kunming, PR China

Received 10 June 2016; received in revised form 21 August 2016; accepted 22 August 2016

Abstract

To address the difficulties on the vibration feature extraction of gear localized faults for rotating machinery under varying speed conditions, an improved narrowband demodulation method with spectrum edit and frequency shift is proposed in the paper. The vibration signal is acquired and resampled at constant angle increments at first, by which the non-stationary signal is converted into a quasi-stationary signal in the angular domain to reduce the distortions caused by the speed fluctuations. Subsequently, the signal in the angular domain is processed by a synchronous average algorithm, where the noises can be eliminated effectively and the order components corresponding to the gear faults become prominent. Finally, the narrowband demodulation scheme with the spectrum edit and frequency shift is applied on the averaged signal. By using the spectrum edit, most of unconcerned components can be filtered out effectively. Moreover, the frequency shift property of the Fourier transform is employed in the proposed demodulation scheme to obtain a better phase demodulation result. Simulations and experiments support the proposed scheme positively.

Keywords: narrowband demodulation, gear faults, spectrum edit, frequency shift, synchronous average

1. Introduction

Gear is one of the most widely used parts in rotating machinery for transmitting power. Meanwhile, it is also a main element where the faults often occur on the running condition of rotating machinery. Thus, gear fault detection has become an important research topic in the field of condition monitoring and faults diagnosis for decades. Most modern techniques for gear fault detection and diagnostics are based on the analysis of vibration signals picked up from the gearbox. The primary target is to detect the presence and type of the gear fault at the early stage when it happens, and then to estimate the machines residual life and to put forward to the corresponding maintenance. Conventional methods for the gear vibration analysis are mainly based on the stationary signal, such as the narrowband demodulation [1], the time synchronous average (TSA) [2], the cepstrum analysis [3], the modulation sidebands analysis [4] etc. However, due to the fluctuating load, the speed fluctuation of rotating machinery is commonly encountered. It makes these conventional methods unsuitable in such condition. For this reason, some researchers have proposed some new methods for gear vibration processing and fault diagnosis under varying speed conditions, such as the extended Kalman filter-based time-varying autoregressive modeling [5], the statistical parameterization [6] and so on. However, these new developed methods are still rarely reported in applications. In contrast, the narrowband demodulation has been studied and widely used for more than 30 years [1]. In viewing of the above-mentioned facts, an improved narrowband demodulation scheme is proposed in this paper to study the gear fault detection of rotating machinery under varying speed conditions.

* Corresponding author. E-mail address: xingwu@aliyun.com
Tel.: +86-871-65930723; Fax: +86-871-65920005

It is well known that the combination of the TSA and the narrowband demodulation analysis is a novel vibration based gear localized faults diagnosis scheme. However, the conventional narrowband demodulation method has two limitations in applications. Firstly, the results from the scheme can be heavily distorted when it is applied to a non-stationary signal, which has time-varying frequency components. Secondly, the conventional phase demodulation scheme originally introduced by McFadden [1] cannot obtain a clear gear fault related phase sharp change feature sometimes. To address these issues, an improvement on the narrowband demodulation analysis for the gear localized faults diagnosis is introduced in the paper. In the improved scheme, the computed order tracking (COT) [7] is employed firstly to convert the non-stationary vibration in the time domain into the quasi-stationary one in the angular domain via the so-called equi-angle resampling scheme, by which the spectral smearing caused by rotating speed fluctuations can be avoided in spectra analysis. Then the synchronous average or rotation domain averaging (RDA) [8] is performed on the resampled data in the angular domain and thus the random noises and other periodic components with non-integer multiple of the period of the reference shaft speed are mostly removed. As a result, the gear localized fault corresponding order components become prominent in the data. In addition, the difficulties in the implementation of the phase demodulation algorithm included in the conventional narrowband demodulation analysis are studied, and the analytic signal model presented in [9] is employed to describe the process of the gear meshing. Lastly, the improved narrowband demodulation scheme is presented, in which the subtraction of the phase contribution by the meshing vibration or carrier component is replaced by the frequency shift algorithm via the properties of the Fourier transform. Instead of the conventional band-pass filtering, a spectral edit based noises and undesired components removal scheme is employed. All these operations ensure that a clear phase demodulation result can be obtained, and thus an improved narrowband demodulation analysis method is achieved for the gear localized fault detection. By combining the COT, the RDA, the new phase demodulation algorithm and the spectral lines edit scheme, the improved scheme owns more advantages on the gear localized fault detection than the conventional narrowband demodulation analysis. Simulations and practical tests show that the proposed scheme is more effective than the conventional methods for the detection of gear localized fault.

2. Brief on Computed Order Tracking

Since the load of machinery may not be a constant in the running condition, the fluctuations of rotating speed are inevitable in rotating machinery. Especially, on the varying speed conditions of rotating machinery, the vibrations generated by the machinery have time-varying frequency characteristics. However, as it is known that a non-stationary signal with the time-varying frequency characteristics does not fit the Fourier transform strictly because it will lead to the so-called frequency blur phenomenon in the spectral plots analysis. To address this issue, the COT scheme has been developed and widely used since 1997 [7]. In theory, the COT plays an important role in converting the non-stationary signal in the time domain into the quasi-stationary one in the angular domain, so that the frequency blur phenomenon can be eliminated. Details of the COT can be found in [7].

3. Signal Synchronous Average

As mentioned above, the TSA is an effective signal pre-processing tool to improve the signal to noise ratio (SNR) in a noisy condition for gear fault detection, which eliminates the interferences unrelated to the rotating speed of the selected reference shaft. Then, the averaged signal is better for spectrum analysis. The principle of the TSA can be briefly descripted as follows.

Given a signal $u(t)$ to simulate the observed vibration from the rotating machinery. By sampling $u(t)$ with a constant time interval Δ, the corresponding discrete version $u(n)$, n=0,1,2, …, N-1 is obtained. Subsequently, to extract the periodic signal components related to the rotating frequency f_r of the reference shaft, $u(n)$ is divided into P data blocks. Assuming M is the number of points in every data block, and $M\Delta$ is an integer multiple of the period T (T=1/f_r) of the synchronising signal, which

is determined by a trigger or synchronizing reference signal phase-locked with the angular position of the reference shaft. Then, the TSA algorithm can be expressed by

$$\bar{u}(m)=\frac{1}{P}\sum_{r=0}^{P-1}u(m-rM) \tag{1}$$

where $\bar{u}(m)$ represents the result after the TSA. Assuming that $u(m)$ includes a periodic component $f(m)$ and a random noise $e(m)$, viz.

$$u(m)=f(m)+e(m) \tag{2}$$

The synchronous averaged signal ū(m) can be expressed by

$$\bar{u}(m)=f(m)+\frac{e(m)}{P} \tag{3}$$

Details of the TSA can be found in [2].

However, it is worth noting that the TSA results can be heavily distorted by the speed fluctuations. For realizing the synchronous average under varying speed conditions, the RDA [8] scheme or synchronous average in the angular domain has been further developed based on the TSA. The brief principle of the RDA can be presented as follows.

Assuming that the observed vibration is $s(t)$ and its corresponding discrete version is $s(n)$, n=0,1,2,…,N-1. By applying the COT on the data series $s(n)$, the equi-angle resampling data series $y(\theta_m)$, m=0,1,2,…,M-1, are obtained, where $\theta_m = m\Omega$, Ω denotes a constant angle increment, M is a multiple of the sampling number per revolution (M is usually the power of two in order to use the fast Fourier transform algorithm).

Thus, the synchronous average in the angular domain can be calculated by

$$\bar{y}(\theta_m)=\frac{1}{P}\sum_{r=0}^{P-1}y(\theta_m-rM),\quad (m=0,\ldots,M-1) \tag{4}$$

where $\bar{y}(\theta_m)$ is the new data series after the synchronous average in the angle domain, P is the total averaging number.

4. Improvement on Narrowband Demodulation

During the running condition of the gearbox, the maximum bending stress is often occurred at the root of gear teeth. If the maximum bending stress exceeds the permissible bending stress, the crack at the root may be produced and then be propagated gradually. In some worst cases, the teeth broken faults may happen, which can cause a huge loss for the mechanical equipment. Then, it is essential to extract gear faults related frequency characteristics for making an evaluation of the running condition of the gearbox. The narrowband demodulation technique is one of widely employed gear fault detection methods. The theory of the conventional narrowband demodulation is presented as follows. Brief on narrowband demodulation

4.1. Brief on narrowband demodulation

From the viewpoint of vibration analysis, the gear meshing frequency component and its harmonics, and the modulation sidebands around the meshing harmonics are the most significant features in the gear faults diagnosis. The modulation sidebands may be caused by transmission errors, speed fluctuations and the gear localized faults etc. For the detection of gear localized faults, the demodulation of the components corresponding to the modulation sidebands is more important, which leads to the birth of the well-known narrowband demodulation analysis [1]. In theory, the modulation phenomenon of a gear vibration includes both amplitude and phase modulations [1]. For constant speed running conditions, the narrowband demodulation technique is a useful tool for analyzing the meshing vibration after the TSA [9], which closely approximates a

truly periodic signal with periodicity in correspondence to one revolution of the analyzed gear when adequate averages are taken [10]. In fact, the TSA can be utilized to eliminate the vibration contributions from other vibration sources in the original picked vibration to a large extent, which includes the background noise and the vibration generated by other rotating parts not mounted on the reference shaft. Meanwhile, the tacho impulse train can be used as a reference signal to determine the angular position of the selected gear. Thus, the modulated gear meshing vibration $x(t)$, which was preprocessed by the TSA, can be expressed as in [1] by

$$x(t)=\sum_{m=0}^{M}A_m\left[1+a_m(t)\right]\cos\left[2\pi f_m t+\beta_m+b_m(t)\right] \tag{5}$$

where the subscript m denotes the mth harmonic of tooth-meshing vibration, A_m is the amplitude, $f_m=m\cdot Z f_r$ (Z is the gear tooth number, f_r denotes the gear rotating frequency and Nf_r represents the fundamental gear meshing frequency), β_m is the initial phase; $a_m(t)$, $b_m(t)$ are the amplitude and phase modulation functions, respectively, which are introduced by the assembly and transmission error, speed fluctuations or other reasons. Since the modulation is periodic with the gear rotating frequency f_r, , those functions can be expressed as in [1] by

$$a_m(t)=\sum_{n=0}^{N}A_{mn}\cos\left(2\pi n f_r t+\alpha_{mn}\right) \tag{6}$$

$$b_m(t)=\sum_{n=0}^{N}B_{mn}\cos\left(2\pi n f_r t+\beta_{mn}\right) \tag{7}$$

where A_{mn} and B_{mn} are amplitudes of the nth harmonic of the mth amplitude and phase modulation functions, respectively.

For a gear localized fault, such as a fatigue crack at the root of one tooth of the gear, it will reduce the mesh stiffness greatly, and then an impact will be produced when the faulty tooth is meshing with other gear. The impact may also introduce extra amplitude and phase modulations to the fault-free gear vibration, where the carrier is the gear meshing frequency and its harmonics. Thus, the gear meshing vibration with a localized fault can be presented as in [9] by

$$y(t)=\sum_{m=0}^{M}A_m\left[1+\tilde{a}_m(t)\right]\cos\left[2\pi f_m t+\beta_m+\tilde{b}_m(t)\right] \tag{8}$$

where $\tilde{a}_m(t)$ and $\tilde{b}_m(t)$ are the modified amplitude and phase modulation functions of the mth harmonic respectively by considering the extra modulations produced by the fault-induced impact. Taking the advantage of the COT for eliminating the frequency blur in the speed fluctuation conditions, the corresponding version of Eq.(8) is modified at the angular domain, which is given by

$$y(\theta)=\sum_{m=0}^{M}A_m\left[1+\tilde{a}_m(\theta)\right]\cos\left[2\pi O_m\theta+\beta_m+\tilde{b}_m(\theta)\right] \tag{9}$$

where θ is the rotating angle of the gear and O_m is the mth order component relating to the meshing frequency of the interesting gear.

In the demodulation progress, the modulation information is extracted from the sidebands around one of main meshing harmonics at first. Then, the averaged signal is band-pass filtered around the selected meshing harmonic with a bandwidth including meaningful number of its sidebands [9]. After the filtering operation, the residual signal $y_m(\theta)$ is used for the demodulation. It is worth mentioning that the interferences between the selected modulation sidebands, and that of neighboring meshing harmonics should be avoided before performing the demodulation.

As in [1], the Hilbert transform [10] is employed to extract both the amplitude signal (envelop signal) $\tilde{a}_m(\theta)$ and the phase signal $\tilde{b}_m(\theta)$ from $y_m(\theta)$. In this study, this can be achieved by constructing the so-called analytic signal $c_m(\theta)=y_m(\theta)+jH[y_m(\theta)]$, where $H[y_m(\theta)]$ denotes the Hilbert transform of $y_m(\theta)$. Then, the amplitude demodulation function $\tilde{a}_m(\theta)$ can be calculated by

$$\tilde{a}_m(\theta)=\frac{\left|c_m(\theta)\right|}{A_m}-1 \tag{10}$$

where the symbol $|\cdot|$ represents absolute value. The phase demodulation function $\tilde{b}_m(\theta)$ can be obtained theoretically as in [1] by

$$\tilde{b}_m(\theta)=\arg\left[c_m(\theta)\right]-\left(2\pi O_m\theta+\beta_m\right) \tag{11}$$

where $\arg[c_m(\theta)]$ denotes the phase angle of $c_m(\theta)$.

4.2. Improvement on band-pass filtering with spectrum edit

For the conventional narrowband demodulation, the band-pass filtering is usually implemented by a standard digital filter. However, the undesired frequency (or order) components cannot be filtered out completely due to the existence of the transition band of a digital band-pass filter, which can distort the demodulation results. To accomplish this issue, the band-pass filter based on the spectrum edit is employed in this paper, in which the spectrum of the vibration signal is edited automatically, viz. the interesting frequency (or order) lines are reserved and others are set to be zeros. The passband W in the order domain is determined by

$$\frac{f_m-\frac{w}{2}\cdot f_r}{f_s}\cdot len\le W\le\frac{f_m+\frac{w}{2}\cdot f_r}{f_s}\cdot len \tag{12}$$

where w denotes the number of the required sidebands around the center frequency f_m, f_s is the sampling frequency, len represents the data length for the inverse fast Fourier transform (IFFT) (it takes the value of power of 2). Note that w is one of the key factors affecting the demodulation results. If the value of w is properly chosen, the filtered signal will carry abundant information related to the gear localized fault. According to [1], the interferences between the modulation sidebands of adjacent meshing harmonics can be totally avoided if $w<(Z-N)$. In this paper, we select w =18 to prevent the demodulation results from the interferences. The selection of w will be a compromise between keeping more interesting sidebands for the accurate demodulation and preventing the inferences from the sidebands of the neighbouring harmonics. Then, the IFFT is utilized to recover the residual signal $y_m(\theta)$ with the reserved order lines.

It should be mentioned that a meshing harmonic with much higher amplitude produces stronger corresponding sidebands and has small interferences from the neighbouring meshing harmonics [1]. Thus, the sidebands carry more modulation information related to the gear localized fault. As a result, the strongest meshing harmonic is often selected as the harmonic for narrowband demodulation.

4.3. Improvement on phase demodulation with frequency shift

Although the standard phase demodulation function can be demodulated by Eq. (11) in theory, the phase demodulation results can be heavily distorted by the noise sometimes. For solving this problem, the frequency shift property of the Fourier transform is used in this paper. The fundamental principle of the proposed phase demodulation is explained as follows.

Assuming that the carrier signal is $x(t) = X\cos(\omega_c t)$ and the phase-modulated function is $p(t)$, then the phase-modulated signal can be expressed by

$$x_p(t) = X\cos[\omega_c t + p(t)] \tag{13}$$

where X and ω_c denote the amplitude and the frequency respectively. To demodulate the modulated phase from $x_p(t)$, the Hilbert transform can be employed to construct the so-called analytic signal, which is defined by

$$\tilde{x}_p(t) = x_p(t) + jH[x_p(t)] \tag{14}$$

where $\tilde{x}_p(t)$ is the analytic signal. The phase information of the single-frequency modulated signal can be expressed by

$$\arg[\tilde{x}_p(t)] = \tan^{-1}\frac{H[x_p(t)]}{x_p(t)} = \omega_c t + p(t) \tag{15}$$

where $\arg[\tilde{x}_p(t)]$ represents the phase function of $x_p(t)$. It is worth mentioning that $\omega_c t$ can also be eliminated by the frequency shift property of the Fourier transform to acquire the phase-demodulated function $p(t)$. It can be expressed by

$$\tilde{x}_p(t)\cdot e^{-\omega_c t} = X\cdot e^{jp(t)} = X\{\cos[p(t)] + j\sin[p(t)]\} \tag{16}$$

and

$$p(t) = \arg\left[\tilde{x}_p(t)\cdot e^{-j\omega_c t}\right] = \tan^{-1}\left\{\frac{\sin[p(t)]}{\cos[p(t)]}\right\} \tag{17}$$

In the same way, for synchronous averaged signal in the angular domain, the aforementioned phase demodulation can also be realized in the order domain. Assuming that $x_p(\theta)$ is the angle-domain version of $x_p(t)$, and its analytic signal $\tilde{x}_p(\theta)$ is obtained by the Hilbert transform, then the phase demodulation based on the frequency shift can be expressed by

$$p(\theta) = \arg\left[\tilde{x}_p(\theta)\cdot e^{-j2\pi O_m\theta}\right] = \tan^{-1}\left\{\frac{\sin[p(\theta)]}{\cos[p(\theta)]}\right\} \tag{18}$$

Eq. (18) means that the modulated-phase θ can be obtained by the frequency shift, which is realized by multiplying $\tilde{x}_p(\theta)$ with $e^{-j2\pi O_m\theta}$ to replace the subtraction in Eq. (11) for the purpose of removing the carrier order (frequency) component (the liner term $2\pi O_m\theta$ according to the frequency shift property of Fourier transform. Compared with Eq. (11), the linear item $2\pi O_m\theta$ is removed before calculating the phase-modulated function $p(\theta)$ in the frequency shift based phase demodulation (see Eq.(11)), which ensures that the gear localized fault can be exposed more accurately. The following simulation and test experiments confirmed that better phase-demodulation results can be achieved by the improvement version.

Note that the narrowband demodulation technique can be effectively performed for the stationary signal. Under the speed fluctuation conditions of rotating machinery, the vibration signal needs to be pre-processed by the RDA to ensure the effect of the narrowband demodulation. The schematic of the proposed narrowband demodulation with frequency shift and spectrum edit is shown in Fig. 1.

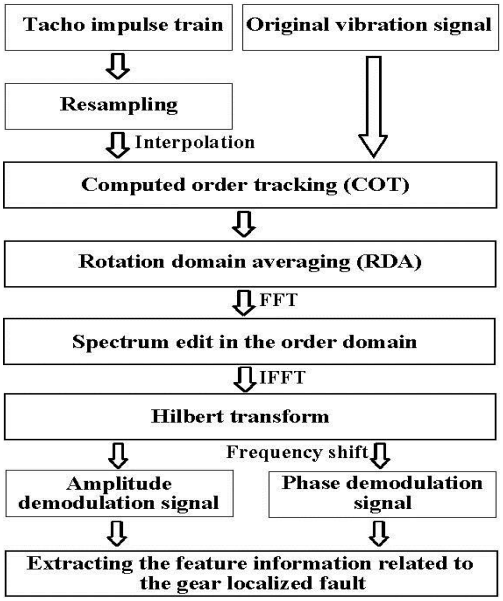

Fig. 1 Schematic of gear fault diagnosis based on narrowband demodulation with spectrum edit and frequency shift

5. Simulation and Test Verification

5.1. Simulation

To verify the efficiency of the proposed method for the gear localized fault detection, simulation studies are first conducted. A tooth-meshing vibration $z(t)$ derived from a faulty gear was simulated, where an impact caused by the gear localized fault near 205° of the shaft angle is introduced, which produces extra modulation effects to Eq. (6) and Eq. (7), respectively. Assuming the impact $d(t)=d_0(t)/\max|d_0(t)|$, and $d_0(t)$ is given as in [9] by

$$d_0(t)=\frac{1}{t\sigma\sqrt{2\pi}}e^{-\frac{(\ln t-\mu)^2}{\sigma^2}} \tag{19}$$

where μ=-6 and σ=0.55. Then, Eq. (6) and Eq. (7) are changed to

$$a'_m(t)=\sum_{n=0}^{N}A_{mn}\cos\left(2\pi nf_r t+\alpha_{mn}\right)-s_a D(t) \tag{20}$$

$$b'_m(t)=\sum_{n=0}^{N}B_{mn}\cos\left(2\pi nf_r t+\beta_{mn}\right)-s_b D(t) \tag{21}$$

where $D(t)$ is the impulse train generated by repeating $d(t)$ once per revolution of the gear shaft, s_a and s_b are coefficients of the impulse train (s_a =1.25 and s_b =1 in the simulation). Moreover, a Gaussian white noise $n(t)$ (power: -15 dBW) is also added, then $z(t)$ can be expressed by

$$z(t)=y(t)+n(t) \tag{22}$$

To simulate the speed fluctuation, the rotating speed (rpm) is given by

$$speed=1200+60\cos\left(0.6\pi t\right) \tag{23}$$

By setting the sampling frequency f_s=40,960 Hz, the observed waveform and the speed profile of the simulated gear are shown in Figs. 2 (a) and 2 (b) respectively.

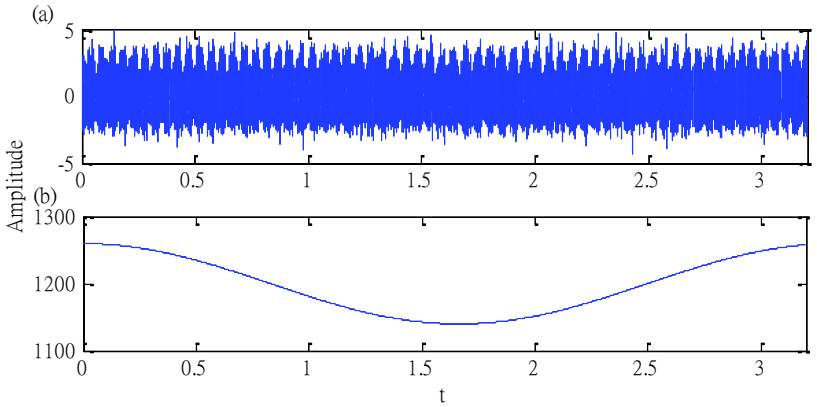

Fig. 2 Simulated vibration: (a) time waveform, (b) speed profile

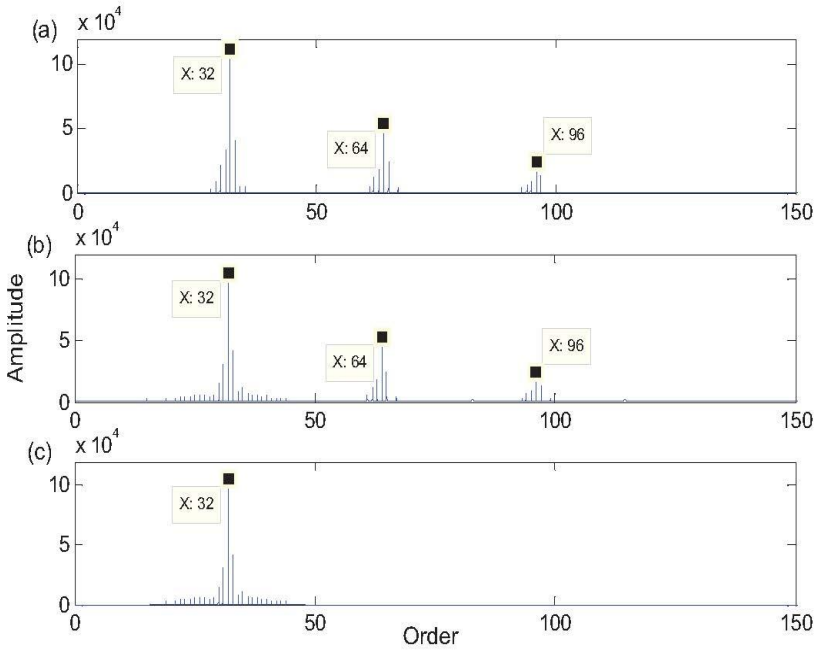

Fig. 3 Order spectra of the simulated vibration:(a) fault-free gear, (b) cracked gear, (c) residual order spectrum after edit

After the RDA, the order spectra of the simulated meshing vibration related with the fault-free gear and the cracked gear are shown in Figs. 3 (a) and 3 (b), respectively. In particular, the gear meshing components (32×, 64×, 96× and its sidebands) can be obviously observed in Fig. 3. The primary 32× and its sidebands are selected for the narrowband demodulation by using the proposed scheme in Fig. 3 (c).

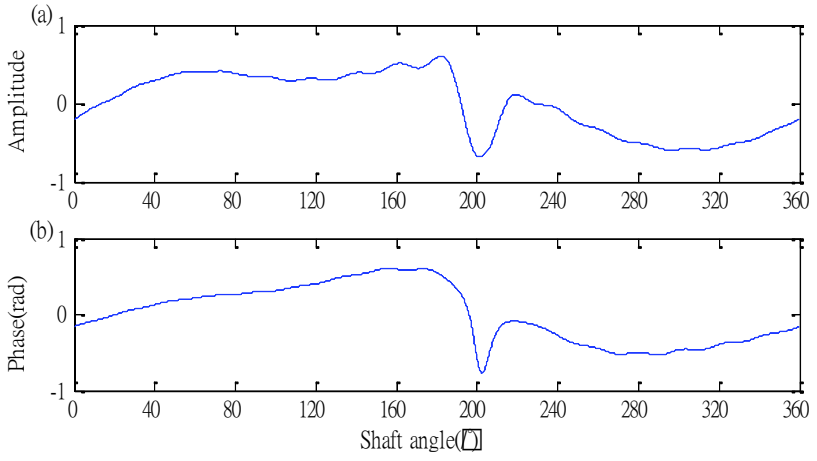

Fig. 4 Results of: (a) amplitude demodulation, (b) phase demodulation

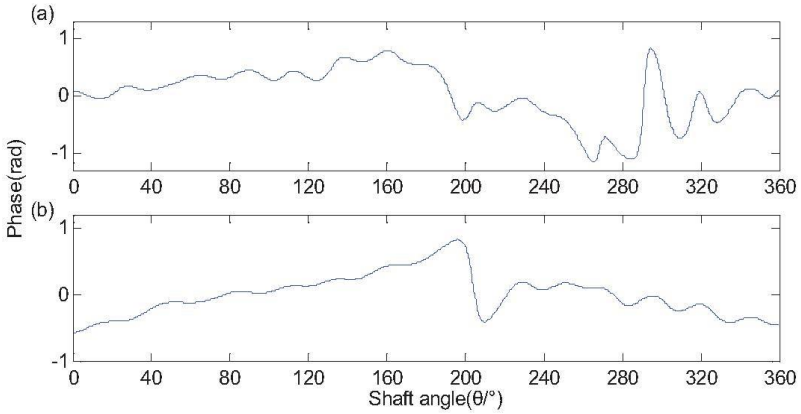

Fig. 5 Phase demodulation results in a noisy condition (additive Gaussian noise power: 15 dBW) by: conventional phase demodulation, (b) improved phase demodulation

The results from the amplitude demodulation and the phase demodulation of the vibration are shown in Figs. 4(a) and 4(b). Two sudden drops can be found at about 205° on both the amplitude demodulation plot and the phase demodulation plot. The plots clearly illustrate the presence of the fault at about 205° of the shaft angle, which corresponds to the simulated gear localized fault feature. By combining the amplitude demodulation and the phase demodulation, the judgment of a gear localized fault is accurate. It should be noted that the above simulation is conducted under a low-noise condition. Fault features can be successfully obtained by using both the conventional and the improved phase demodulation algorithms. However, in a noisy condition, the two phase demodulation approaches may obtain different results. For example, when the power of Gaussian noise in Eq. (22) was increased to 15 dBW, the phase demodulation results of the two demodulation schemes are showed in Figs. 5(a) and 5(b), respectively. Obviously, the conventional phase demodulation method is invalid, while the improved version can still get a satisfactory result. The difference can be explained as that the phase of the whole signal is calculated at first by arctangent function in the conventional phase demodulation (see Eq. (11)), then the liner term $2\pi O_m \theta$ is subtracted to get the modulation phase. The phase calculation of the whole signal can be distorted by possible disturbances. On the contrary, in the improved method the liner term is removed by the frequency shift at first, and then used to directly calculate the modulation phase, which ensures more accurate result. These results demonstrate that the improved narrowband demodulation scheme is robust for exposing the existence of localized gear faults.

5.2. Test

To verify the validity of the proposed method to the real-world data, tests have been done on a gearbox test rig, in which the driven gear includes a crack at the root of one tooth of the wheel mounted. In reality, before mounting the driven gear on the testing machine, the gear was cut a thin groove at the root of a gear tooth by the electrical discharge machining (EDM) to simulate a real fatigue crack. The vibration was picked up at the bearing house of the gearbox by means of NI 9215 acquisition card (four channels simultaneous sampling) with a DH112 acceleration sensor shown in Fig. 6(a). Meanwhile, the tacho impulse train provided by an eddy probe was also acquired simultaneously for obtaining the speed profile.

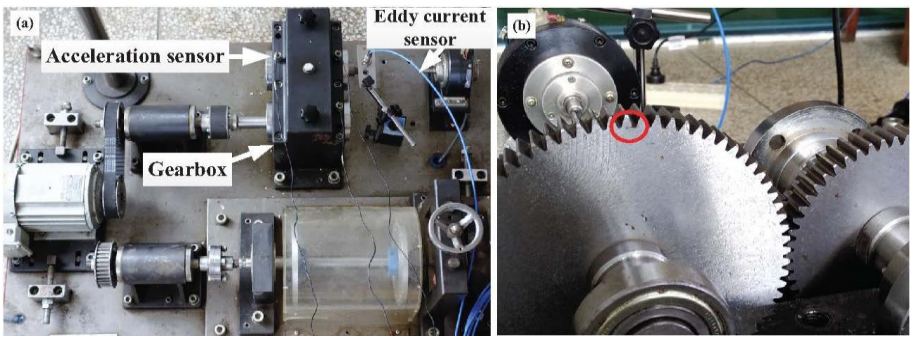

Fig. 6 Test rig: (a) gearbox and, (b) a crack at the root of the driven gear

Some experiment parameters are listed as follows: the teeth number of the driving gear and the driven gear are 55 and 75, respectively; the rotating speed of the pinion is run around 160 to 600 rpm; the sampling ratio is set as 102.4 kHz, and the sensitivity of the accelerometer and the probe are 5.20 pC/g and 2.5 V/mm, respectively.

The proposed narrowband demodulation scheme was implemented. The measured signals (Fig. 7) are preprocessed and analyzed by means of the LabVIEW and MATLAB. Firstly, the resampling time marks are estimated in accordance with the reference shaft or output shaft (the driven gear mounted on it). Then, the raw vibration is converted into the angle-domain one by resampling at a constant angle increment or 2,048 points per revolution. Subsequently, the RAD is carried out to remove the interferences generated by other sources that are different from the interesting gear. The order spectrum is shown in Fig. 8 (a), in which the first meshing harmonic (75×) is more prominent. Then, the 75× and its sidebands are selected for the filtering by using the spectrum edit approach. By reserving the 75× and its modulation sidebands, setting other order lines to zeros, the angle-domain signal is recovered by performing the IFFT on the edited order spectrum. The edited order spectrum and corresponding recovered signal are shown in Figs. 8(b) and 8(c), respectively. Finally, the demodulation with the frequency shift approach is performed according to the above-mentioned theory.

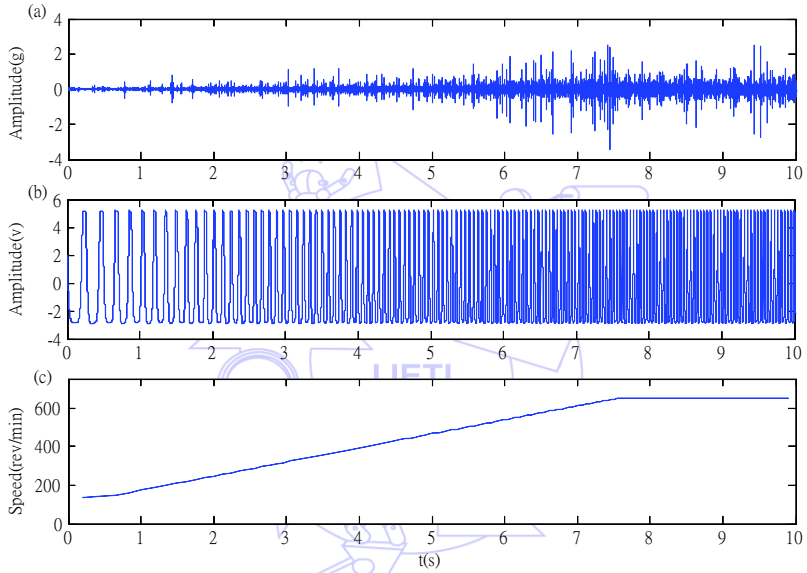

Fig. 7 Measured signals: (a) raw vibration, (b) tacho impulse train, (c) speed profile

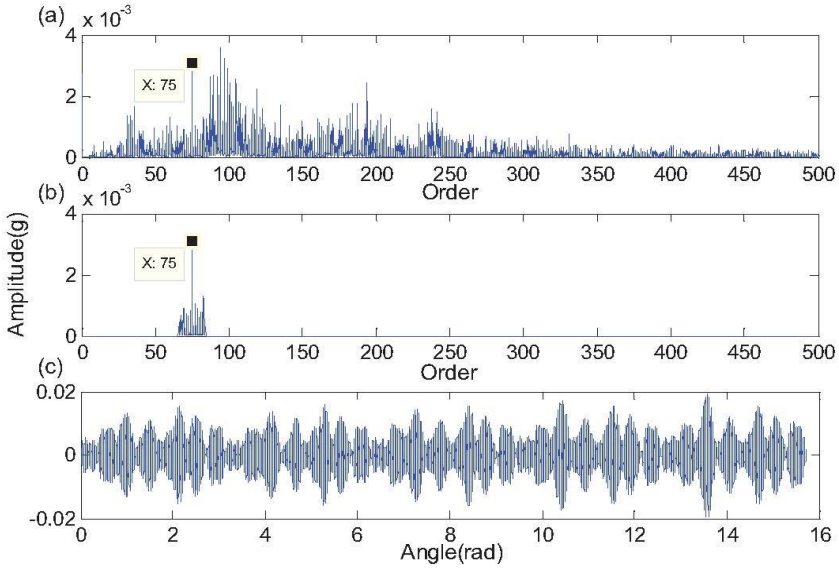

Fig. 8 Filtering by spectrum edit: (a) order spectrum of vibration after RDA, (b) order spectrum after spectrum edit, (c) recovered signal in the angular domain after spectrum edit

The comparative demodulation results between the conventional approach and the improved version are shown in Fig. 9. The minimum value can be found at about 224° according to the reference shaft angle shown in Fig. 9(a). We found that the difference of the amplitude demodulation plots between the conventional version and the improved version is not significant, then only one plot from the improved version is shown in Fig. 9(a), and it cannot reflect the gear localized fault clearly. The phase demodulation results provided by the conventional approach and the proposed improved version are shown in Figs. 9(b) and 9(c). It is clearly shown that the phase change can be found at almost the same angle in Figs. 9(b) and 9(c). However, the result from the improved phase demodulation scheme is obviously better than that of the conventional phase demodulation algorithm presented in Eq. (11). The results from actual tests validate again that the improved narrowband demodulation scheme is superior to the conventional narrowband demodulation approach.

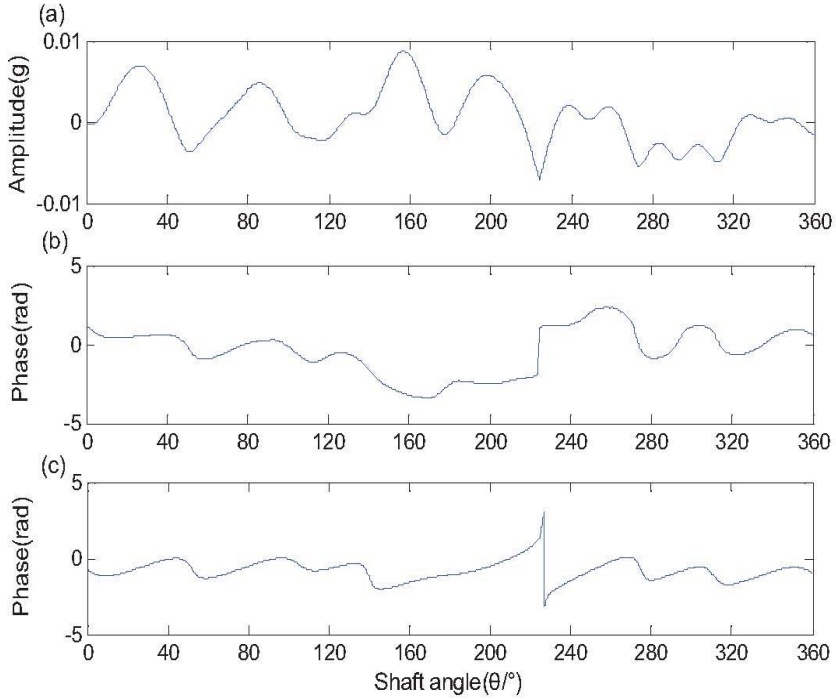

Fig. 9 Narrowband demodulation results: (a) amplitude demodulation, (b) conventional phase demodulation, (c) improved phase demodulation

6. Conclusions

By combining the COT, the RDA and the conventional narrowband demodulation, an improved narrowband demodulation scheme has been studied for the localized gear faults diagnosis. The distortion caused by the speed fluctuations can be reduced by the COT. Instead of the standard digital band-pass filtering and the direct subtraction in the phase demodulation, the spectrum edit approach and the frequency shift approaches are used, and thus the deficiencies of the conventional narrowband demodulation can be eliminated. Localized gear faults corresponding features can be clearly exposed in the demodulation results by using the proposed scheme. Simulations and tests validate the superiority of the proposed approach.

Acknowledgements

Project supported by the National Science Foundation of China (Grant no. 51365023) and (Grand no. 51675251).

References

[1] P. D. McFadden, "Detecting fatigue cracks in gears by amplitude and phase demodulation of the meshing vibration," Journal of Vibration and Acoustics, vol. 108, pp. 165-170, Apr. 1986.

[2] P. D. McFadden, "A revised model for the extraction of periodic waveforms by time-domain averaging," Mechanical Systems and Signal Processing, vol. 1, pp. 83-95, Jan. 1987.
[3] R. B. Randall, "Cepstrum analysis and gearbox fault diagnosis," Bruel & Kjaer: Application Notes, 1980.
[4] M. Inalpolat and A. Kahraman, "A theoretical and experimental investigation of modulation sidebands of planetary gear sets," Journal of Sound and Vibration, vol. 323, pp. 677-696, June 2009.
[5] Y. Shao and C. K. Mechefske, "Gearbox vibration monitoring using extended Kalman filters and hypothesis tests," Journal of Sound and Vibration, vol. 325, pp. 629-648, Aug. 2009.
[6] J. McBain and M. Timusk, "Fault detection in variable speed machinery: Statistical parameterization," Journal of Sound and Vibration, vol. 327, pp. 623-646, Nov. 2009.
[7] K. R. Fyfe and E. D. S. Munck, "Analysis of computed order tracking," Mechanical Systems and Signal Processing, vol. 11, pp. 187-205, Mar. 1997.
[8] C. J. Stander, P. S. Heyns, and W. Schoombie, "Using vibration monitoring for local fault detection on gears operating under fluctuating load conditions," Mechanical Systems and Signal Processing, vol. 16, pp. 1005-1024, Nov. 2002.
[9] W. Wang, "Early detection of gear tooth cracking using the resonance demodulation technique," Mechanical Systems and Signal Processing, vol. 15, pp. 887-903, Sep. 2001.
[10] G. Dalpiaz, A. Rivola, and R. Rubini, "Effectiveness and sensitivity of vibration processing techniques for local fault detection in gears," Mechanical Systems and Signal Processing, vol. 14, pp. 387-412, May 2000.